University of Reading

Cloud feedback uncertainty in the equatorial Pacific across CMIP6 models

Article

Published Version

Creative Commons: Attribution 4.0 (CC-BY)

Open Access

Hill, P. G. ORCID: https://orcid.org/0000-0002-9745-2120, Finney, D. L. ORCID: https://orcid.org/0000-0002-3334-6935 and Zelinka, M. D. ORCID: https://orcid.org/0000-0002-6570-5445 (2025) Cloud feedback uncertainty in the equatorial Pacific across CMIP6 models. Geophysical Research Letters, 52 (19). e2025GL117183. ISSN 1944-8007 doi: 10.1029/2025gl117183 Available at https://centaur.reading.ac.uk/125321/

It is advisable to refer to the publisher's version if you intend to cite from the work. See Guidance on citing.

To link to this article DOI: http://dx.doi.org/10.1029/2025gl117183

Publisher: American Geophysical Union

All outputs in CentAUR are protected by Intellectual Property Rights law, including copyright law. Copyright and IPR is retained by the creators or other copyright holders. Terms and conditions for use of this material are defined in the End User Agreement.

www.reading.ac.uk/centaur

University of Reading

CentAUR

Central Archive at the University of Reading

Reading's research outputs online

Check for updates

AGU ADVANCING EARTH AND SPACE SCIENCES

Geophysical Research Letters

RESEARCH LETTER
10.1029/2025GL117183

Cloud Feedback Uncertainty in the Equatorial Pacific Across CMIP6 Models

Peter G. Hill[1,2], **Declan L. Finney**[3], **and Mark D. Zelinka**[4]

[1]Department of Meteorology, University of Reading, Reading, UK, [2]Now at European Centre for Medium-Range Weather Forecasts, Reading, UK, [3]School of Earth and Environment, University of Leeds, Leeds, UK, [4]Lawrence Livermore National Laboratory, Livermore, CA, USA

Abstract Cloud feedback is the largest uncertainty in estimating Equilibrium Climate Sensitivity. In this study we focus on the equatorial Pacific, where CMIP6 model cloud feedback spread is notably large. Cloud radiative effects in this region are relevant for the global climate. Our findings show that models predict a consistent shift towards the ascent regime in response to El Nino-like sea surface warming. Models diverge in terms of the radiative impact due to differences in cloud characteristics in ascent and subsidence regimes. Using the observed relationship between circulation regime and cloud radiative effect, we find a reduction in the regional mean cloud feedback estimate from 0.77 to 0.22 W m^{-2} K^{-1}, though this does not substantially lessen the model spread in total feedback. Pathways to reduce this spread include: improving confidence in the regional ocean warming pattern, and using observations and models to understand cloud type and circulation interactions.

Plain Language Summary The radiative response of clouds to warming, that is, their feedback, represents the biggest uncertainty in predicting how much the Earth as a whole will warm as greenhouse gases increase. This study focuses on the equatorial Pacific, where climate models show significant differences in cloud feedback estimates. Clouds in this region, particularly through their role in the El Nino phenomenon, are important for global climate. Our research shows that, for a given model, the more sea surface temperatures warm in the Eastern Pacific, the larger a shift to convective circulations. However, models vary in their predictions of the properties of the clouds that form under different circulations, and therefore what radiative effect can be expected with such a change in circulation. By using the observed relationship between cloud radiative effect and circulation regime, this study reduces the estimated cloud feedback in the region from 0.77 to 0.22 W m^{-2} K^{-1}, but this does not reduce the size of differences between models. To improve cloud feedback predictions, future work should focus on better understanding regional ocean warming patterns and cloud behavior in relation to atmospheric circulation.

Key Points:

- The equatorial Pacific shows particularly large spread in cloud feedback in coupled models but not atmosphere-only models
- Model spread in circulation regime-dependent cloud radiative effects is a major cause of spread in dynamic cloud feedback
- Using observed regime-dependent cloud radiative effect as a constraint reduces the regional mean feedback from 0.77 to 0.21 W m^{-2} K^{-1}

Supporting Information:

Supporting Information may be found in the online version of this article.

Correspondence to:

D. L. Finney,
d.l.finney@leeds.ac.uk

Citation:

Hill, P. G., Finney, D. L., & Zelinka, M. D. (2025). Cloud feedback uncertainty in the equatorial Pacific across CMIP6 models. *Geophysical Research Letters*, *52*, e2025GL117183. https://doi.org/10.1029/2025GL117183

Received 30 SEP 2024
Accepted 26 SEP 2025

Author Contributions:

Conceptualization: Peter G. Hill, Declan L. Finney
Data curation: Mark D. Zelinka
Formal analysis: Peter G. Hill, Declan L. Finney
Funding acquisition: Peter G. Hill, Declan L. Finney
Writing – original draft: Peter G. Hill, Declan L. Finney
Writing – review & editing: Peter G. Hill, Declan L. Finney, Mark D. Zelinka

© 2025. The Author(s).
This is an open access article under the terms of the Creative Commons Attribution License, which permits use, distribution and reproduction in any medium, provided the original work is properly cited.

1. Introduction

Despite the clear and increasingly urgent need for accurate climate predictions, even the equilibrium global mean temperature increase arising from a doubling of carbon dioxide concentrations (known as the equilibrium climate sensitivity [ECS]) remains highly uncertain (Arias et al., 2021; Meehl et al., 2020). This uncertainty is in large part caused by uncertainty in the response of clouds to warming, which are known as cloud feedbacks (Forster et al., 2021; Zelinka et al., 2020). Feedbacks in tropical clouds are particularly uncertain (Sherwood et al., 2020).

It is becoming clear that climate models alone are not appropriate for constraining ECS, and a wider evidence base must be used, as demonstrated by Sherwood et al. (2020). However, global climate models remain vital tools for predicting the impact of climate change on quantities relevant to human activity, such as precipitation, surface temperature, and occurrence of severe weather events (e.g., Di Sante et al., 2021). Since many of these changes are dependent on the models' ECS, it is crucial to understand the differences in climate sensitivity between the models, which are primarily driven by differences in cloud feedbacks (Zelinka et al., 2020).

Much of the uncertainty in cloud feedbacks arises from the fact that clouds are complex and highly dynamic phenomena. In particular, the impact that a change in one cloud property has on the cloud radiative effects depends on the other properties of the cloud and the surrounding environment (McKim et al., 2024). To reduce this complexity, research efforts often focus on a specific cloud type or change (e.g., Sokol et al., 2024; M. J. Webb et al., 2015; Zelinka & Hartmann, 2011). This has led to significant progress in understanding cloud feedbacks

19448007, 2025, 19, Downloaded from https://agupubs.onlinelibrary.wiley.com/doi/10.1029/2025GL117183 by NICE, National Institute for Health and Care Excellence, Wiley Online Library on [28/10/2025]. See the Terms and Conditions (https://onlinelibrary.wiley.com/terms-and-conditions) on Wiley Online Library for rules of use; OA articles are governed by the applicable Creative Commons License

(Sherwood et al., 2020). However, climate model spread has shown little reduction (Zelinka et al., 2020). In this study we take a different approach, focusing on the differences between climate model cloud feedbacks in a specific region. This approach provides a different perspective from the widely used focus on specific cloud types, and enables different analysis methods to be used. Moreover, focusing on cloud feedbacks within a specific region may provide insight into how feedbacks from different cloud types are correlated with each other. Regional differences in cloud feedbacks are also important to understand as both a tracer and contributor to circulation changes which may affect local and teleconnected weather. Motivated by these ideas and by analysis of how the inter-model standard deviation of cloud feedbacks in climate models varies with location (see Section 3), this study focuses specifically on the causes of differences in cloud feedbacks between climate models in the equatorial Pacific, which we define as the region bounded by 160°E–270°E and 10°S–10°N.

This region has received a lot of attention due to the well documented teleconnections of El Nino and consequent societal impacts (e.g., Alizadeh, 2023). Additional motivation is provided by the broadly consistent shift towards an El Nino-like state under future warming (Erickson & Patricola, 2023; Heede & Fedorov, 2023; Shin et al., 2022) in the 6th Coupled Model Intercomparison Project (CMIP6) models. Given the known strong El Nino-clouds-circulation coupling (Middlemas et al., 2019; Rädel et al., 2016), it is imperative to characterize and understand the response of equatorial Pacific cloud feedbacks. Bock and Lauer (2024) considered the Pacific ITCZ in their analysis of low, mid, and high ECS CMIP models. Their Figure 7d showed a correspondence between the cloud feedbacks in the region and model variability in global ECS. The results we will present add impetus to investigate cloud feedbacks in the equatorial Pacific, provide a focused analysis of CMIP6 model cloud feedback variability, and offer insights into the causes of this variability.

2. Methods

This study focuses on the latest generation of CMIP6 models and includes both coupled atmosphere-ocean and atmosphere-only simulations. The study includes 45 models for which comparable piControl and abrupt4xCO_2 simulations are available with one ensemble member for each model, as listed in Table S1 in Supporting Information S1. In addition to these coupled atmosphere-ocean simulations, we study cloud feedbacks in an atmosphere-only configuration for 10 models which also provide AMIP-p4K simulations and the diagnostics required to compute cloud feedbacks using cloud radiative kernels (i.e., ISCCP simulator output), as indicated in Table S1 in Supporting Information S1.

Total cloud feedbacks, computed as the adjusted change in cloud radiative effect (CRE) via radiative kernels, are taken from Zelinka et al. (2020), including additional models that populated the CMIP6 archive post-publication (Zelinka, 2022, 2024). Atmosphere-only cloud feedbacks are computed using the cloud radiative kernel approach Zelinka et al. (2012). An assessment of feedback estimation methodology is discussed in Text S1 in Supporting Information S1. Cloud feedbacks in both the coupled and atmosphere-only experiments are further separated into those due to low clouds and those due to non-low clouds following the breakdown advocated in Zelinka et al. (2016). For the atmosphere-only feedbacks that are estimated using cloud radiative kernels, this is done by considering only low (cloud top pressures >680 hPa) or non-low (cloud top pressures <680 hPa) bins of the cloud fraction histogram in the calculation. For the coupled model cloud feedbacks, Zelinka et al. (2020) used the M. J. Webb et al. (2006) decomposition which distinguishes low and non-low cloud feedbacks based on the relative strength of longwave and shortwave radiation anomalies. Low and non-low cloud feedbacks estimated via the M. J. Webb et al. (2006) decomposition agree closely with those computed using the Zelinka et al. (2016) method for the 11 models for which ISCCP simulator output is available in Zelinka et al. (2020).

Cloud feedbacks can be further decomposed into dynamic, thermodynamic, and co-variation components (Bony et al., 2004; Wyant et al., 2006) as given by the following equation

$$\delta\bar{C} = \underbrace{\int_{-\infty}^{\infty} C(\omega)\delta P(\omega)d\omega}_{\text{dynamic}} + \underbrace{\int_{-\infty}^{\infty} \delta C(\omega)P(\omega)d\omega}_{\text{thermodynamic}} + \underbrace{\int_{-\infty}^{\infty} \delta C(\omega)\delta P(\omega)d\omega}_{\text{co-variation}}, \quad (1)$$

where C(ω) is the net CRE as a function of the 500 hPa vertical velocity, P(ω) is the PDF of the 500 hPa vertical velocity, and δC(ω) and δP(ω) represent the changes in the CRE and PDF of ω500 under climate change.

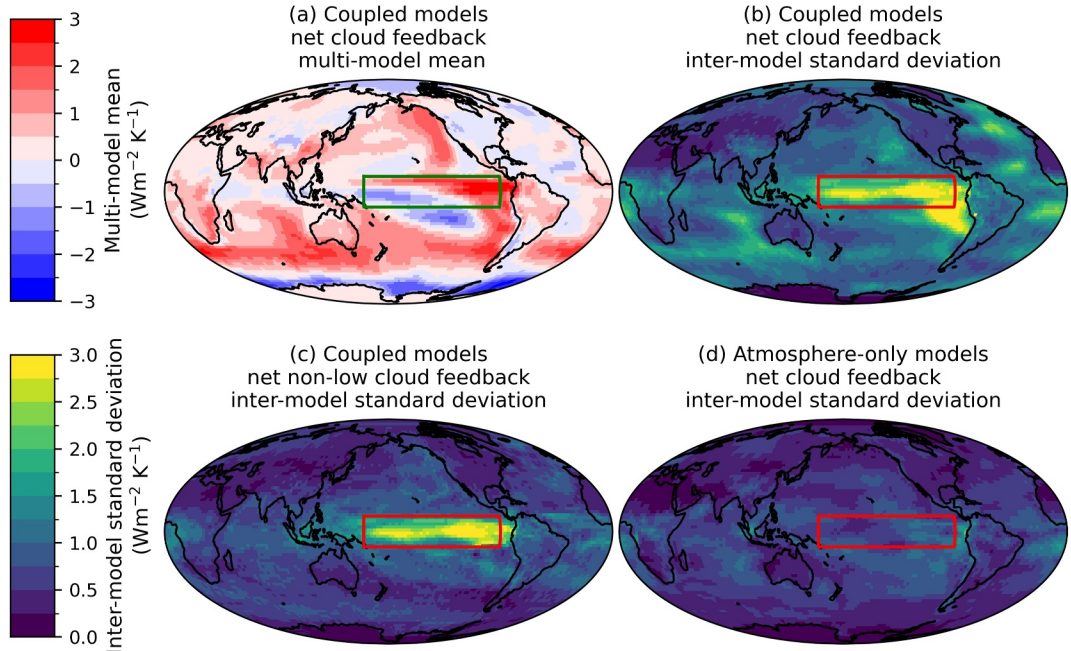

Figure 1. Multi-model mean and inter-model standard deviations of net cloud feedback. (a, b) Are based on 45 atmosphere-ocean coupled simulations, (c) shows the net non-low cloud feedback standard deviation for the same 45 simulations, and (d) shows the net cloud feedback standard deviation for 10 atmosphere-only simulations.

For the purposes of this article, the thermodynamic and co-variation terms are combined into a single term, which we shall henceforth refer to as the non-dynamic cloud feedback. This new non-dynamic term is calculated as the difference between the total and dynamic cloud feedbacks, which enables us to calculate cloud feedback components that are consistent with the kernel derived total cloud feedback without recalculating the kernels as a function of the 500 hPa vertical velocity that is,

$$\delta\bar{C} = \underbrace{\int_{-\infty}^{\infty} C(\omega)\delta P(\omega)d\omega}_{\text{dynamic}} + \underbrace{\left(\delta\bar{C} - \int_{-\infty}^{\infty} C(\omega)\delta P(\omega)d\omega\right)}_{\text{non-dynamic}}, \quad (2)$$

These calculations are based on monthly mean data with all models regridded to a fixed 2° latitude-longitude grid. A 2 hPa day^{-1} bin width is used for the 500 hPa vertical velocity. Observed CRE as a function of the 500 hPa vertical velocity is calculated based on averaging the combination of CERES-EBAF satellite observations (Loeb et al., 2018) with three different reanalyses (ERA5; (Hersbach et al., 2020), JRA55; (Kobayashi et al., 2015), and MERRA2; (Gelaro et al., 2017)), as described by Hill et al. (2023).

3. Climate Model Cloud Feedbacks in the Equatorial Pacific

Figure 1 shows the multi-model mean (Figure 1a) and inter-model standard deviation (Figures 1b–1d) of cloud feedbacks in the latest generation of climate models, CMIP6. Net cloud feedbacks are particularly large in the equatorial Pacific (Figure 1a), which has been the case for several generations of climate models (Ceppi et al., 2017; Soden & Vecchi, 2011). Even more remarkable is the inter-model standard deviation of net cloud feedback in this region (Figure 1b), which, along with the southeast subtropical Pacific, is notably larger than elsewhere in the globe. Whilst the southeast region is dominated by low cloud feedback variability, and is well characterized under the marine low-cloud feedback (Sherwood et al., 2020), the large variability in net cloud feedback within the equatorial Pacific is primarily due to non-low clouds (Figure 1c). The non-low cloud feedback characterization is ambiguous in terms of its potential drivers and therefore warrants further investigation. Atmosphere-only experiments have much lower variability in cloud feedback in this region (Figure 1d).

19448007, 2025, 19, Downloaded from https://agupubs.onlinelibrary.wiley.com/doi/10.1029/2025GL117183 by NICE, National Institute for Health and Care Excellence, Wiley Online Library on [28/10/2025]. See the Terms and Conditions (https://onlinelibrary.wiley.com/terms-and-conditions) on Wiley Online Library for rules of use; OA articles are governed by the applicable Creative Commons License

19448007, 2025, 19, Downloaded from https://agupubs.onlinelibrary.wiley.com/doi/10.1029/2025GL117183 by NICE, National Institute for Health and Care Excellence, Wiley Online Library on [28/10/2025]. See the Terms and Conditions (https://onlinelibrary.wiley.com/terms-and-conditions) on Wiley Online Library for rules of use; OA articles are governed by the applicable Creative Commons License

Moreover, the coupled equivalents of these atmosphere-only simulations do have similar variability to the full set of coupled models (Figure S1 in Supporting Information S1).

For the coupled models considered in this study, the multi-model mean net cloud feedback in this region is 0.77 W m^{-2} K^{-1}, with an inter-model standard deviation of 1.33 W m^{-2} K^{-1}. Since this region occupies 5.3% of the earth's area, this region contributes ∼0.04 W m^{-2} K^{-1} to the global mean cloud feedback, with an inter-model standard deviation of 0.07 W m^{-2} K^{-1}. This represents ∼19% of the inter-model standard deviation in global mean cloud feedback (0.38 W m^{-2} K^{-1}) and is as large as the inter-model standard deviation in cloud feedback for the majority of individual cloud types in CMIP6 (Zelinka et al., 2022). Models are known to exhibit notable differences in the location of changes to the ITCZ within the Pacific region. However since these occur within our domain the effect is averaged out (Figure S2 in Supporting Information S1), and changes in ITCZ location do not contribute to the model feedback spread presented here. Moreover, the domain mean cloud feedback for this region is only weakly linked to cloud feedbacks outside the region (Figure S3 in Supporting Information S1). Alternative domain bounds were tested using ±20° latitude, and additionally 130°W for the western edge. High correlation between model domain-mean feedback in the original and new domains showed that results are not sensitive to domain definition.

This region has previously been highlighted as an exception to the high correlations seen between cloud radiative feedbacks in atmosphere-only and coupled atmosphere-ocean simulations across both CMIP5 and CMIP6 models (Qin et al., 2022), which was attributed to differences in SST and ω500. This motivates decomposing the cloud feedbacks in this region into dynamic and non-dynamic components (Bony et al., 2004; Byrne & Schneider, 2018). Moreover, these differences suggest that (atmosphere-only) process models that may be used to study tropical cloud feedbacks (e.g., Mackie & Byrne, 2023; Sokol et al., 2024; Stauffer & Wing, 2022; Wing et al., 2020) may be missing a significant dynamic feedback component linked to changes in SST patterns.

4. Causes of Equatorial Pacific Feedback Variability

As detailed in the methodology, cloud feedbacks in this region are decomposed into dynamic and non-dynamic components for each model (Figure 2a). The coupled models show a wide spread in both the dynamic and non-dynamic components. Qin et al. (2022) hypothesized that the dynamic component was the main driver of poor correlation between coupled and atmosphere-only models in the tropical Pacific. However, we find that correlation between coupled and atmosphere-only versions of models is not significant at 5% level for either dynamic (0.60) or non-dynamic (0.35) components. Both the lack of correlation between the thermodynamic feedbacks and the smaller variability in the atmosphere-only cloud feedbacks are partially due to differences in local SST. As a result the atmosphere-only models are less useful for understanding the spread in the coupled models

Both dynamic and non-dynamic components of the cloud feedback show large spread in the coupled models. Previous studies have found that spread in net dynamic cloud feedback is much smaller than the spread in net non-dynamic cloud feedback in both idealized models (e.g., Mackie & Byrne, 2023) and climate models over the entire tropics (e.g., Hill et al., 2023). However, circulation changes with warming in smaller regions such as the equatorial Pacific are not expected to balance; increased ascent in this region may be balanced by increased subsidence in another region. It is, therefore, important to consider the dynamic cloud feedback when looking to understand regional cloud feedbacks. Consequently, in this study we focus on controls of the dynamic cloud feedback spread in coupled models. The focus on dynamic feedback is also motivated by work finding that tropical ascent fraction changes with warming (Su et al., 2020). Mackie and Byrne (2023) also find that changes in ascent fraction provides an important control on dynamic cloud feedback in a set of cloud resolving models. In this study, we take the opportunity to investigate whether the dynamic feedback and its controls play a role in a region of high cloud feedback spread across CMIP6 models.

In all models, the dynamic cloud feedback has a positive contribution from subsidence regimes (Figure 2b), with the frequency of the most commonly occurring weak subsidence regimes (Figure S4 in Supporting Information S1) predicted to decrease in frequency in all models (Figure 2c). This is countered by a negative contribution from ascent regimes, which are predicted to increase in frequency in all models (Figures 2b and 2c). Figure 2d suggests that the sign of the dynamic cloud feedback is strongly related to the net CRE, in particular the difference between the net CRE in ascent and subsidence regimes (CRE_{asc}-CRE_{sub}). The upper tercile of models, based on their dynamic feedback component, have a more negative net CRE in subsidence regimes than in ascent regimes

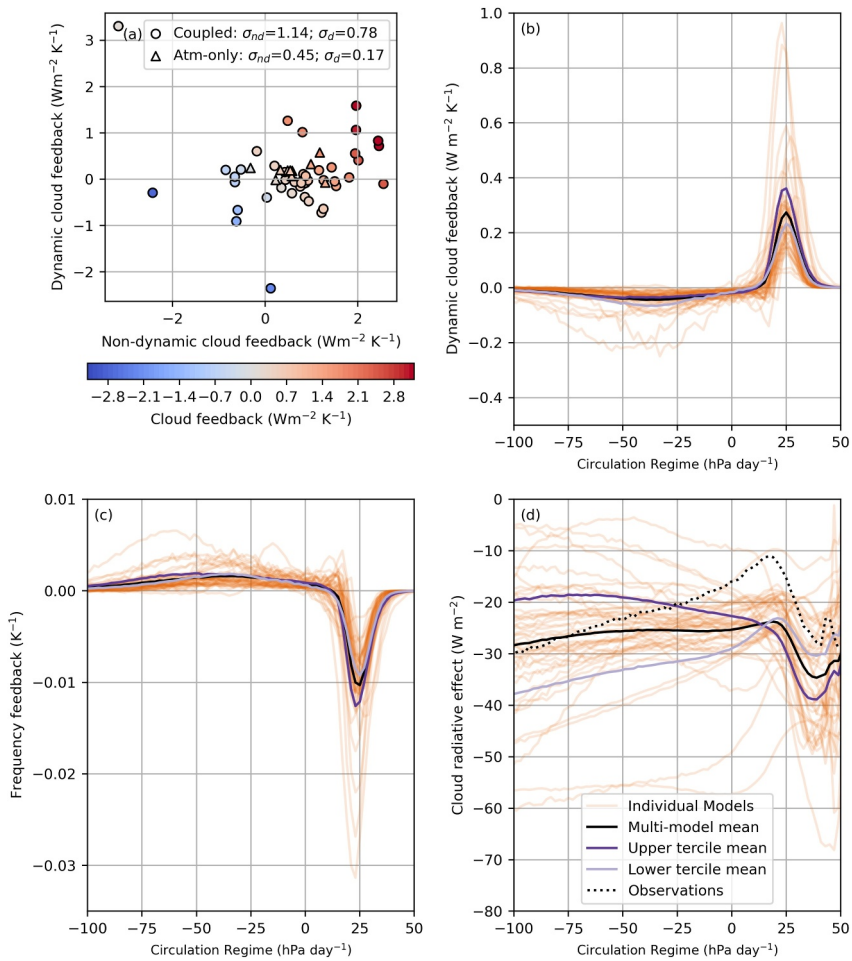

Figure 2. (a) Dynamic ("d") and non-dynamic ("nd") cloud feedbacks for the region bounded by 160°E–270°E and 10°S–10°N for each of the coupled (circles) and atmosphere-only (triangles) models listed in Table S1 in Supporting Information S1. Color of the circles and triangles indicates the total cloud feedback (dynamic + non-dynamic) for that model. (b–d) Dynamic cloud feedback, global mean surface temperature normalized change in circulation regime frequency, and net Cloud Radiative Effect (CRE) as a function of 500 hPa vertical velocity for the coupled models. Observations in panel (d) are based on a combination of CERES-EBAF satellite observations of CRE and reanalyses estimates of 500 hPa vertical velocity (see Section 2). Panel (b) is the product of panels (c, d). Model tercile groupings for all plots are based on the dynamic cloud feedback. The SW and LW equivalents of panel (d) are shown in Figure S8 in Supporting Information S1.

(Figure 2d), so that the shift from subsidence to ascent increases the net CRE and gives a positive dynamic feedback. On the other hand, the lower tercile of models have a less negative CRE in subsidence regimes than in ascent regimes so that the shift from subsidence to ascent causes a decrease in net CRE and gives a negative dynamic cloud feedback. The lower tercile results are more consistent with the observations which show a maximum in the net CRE around 20 hPa day^{-1} (Figure 2d) and a more negative net CRE in ascent regimes. Net CRE differences between the two terciles are primarily driven by SW CRE differences (Figure S8 in Supporting Information S1) with increased magnitude SW CRE for ascending regimes for the lower tercile.

This contrast between the net CRE for the two different terciles suggests that it may be possible to approximate the dynamic cloud feedback simply by focusing on the change in ascent fraction (Δ_{asc}; note that $\Delta_{asc} = -\Delta_{sub}$ so either could be used) and CRE$_{asc}$-CRE$_{sub}$, which can be expressed mathematically as

19448007, 2025, 19, Downloaded from https://agupubs.onlinelibrary.wiley.com/doi/10.1029/2025GL117183 by NICE, National Institute for Health and Care Excellence, Wiley Online Library on [28/10/2025]. See the Terms and Conditions (https://onlinelibrary.wiley.com/terms-and-conditions) on Wiley Online Library for rules of use; OA articles are governed by the applicable Creative Commons License

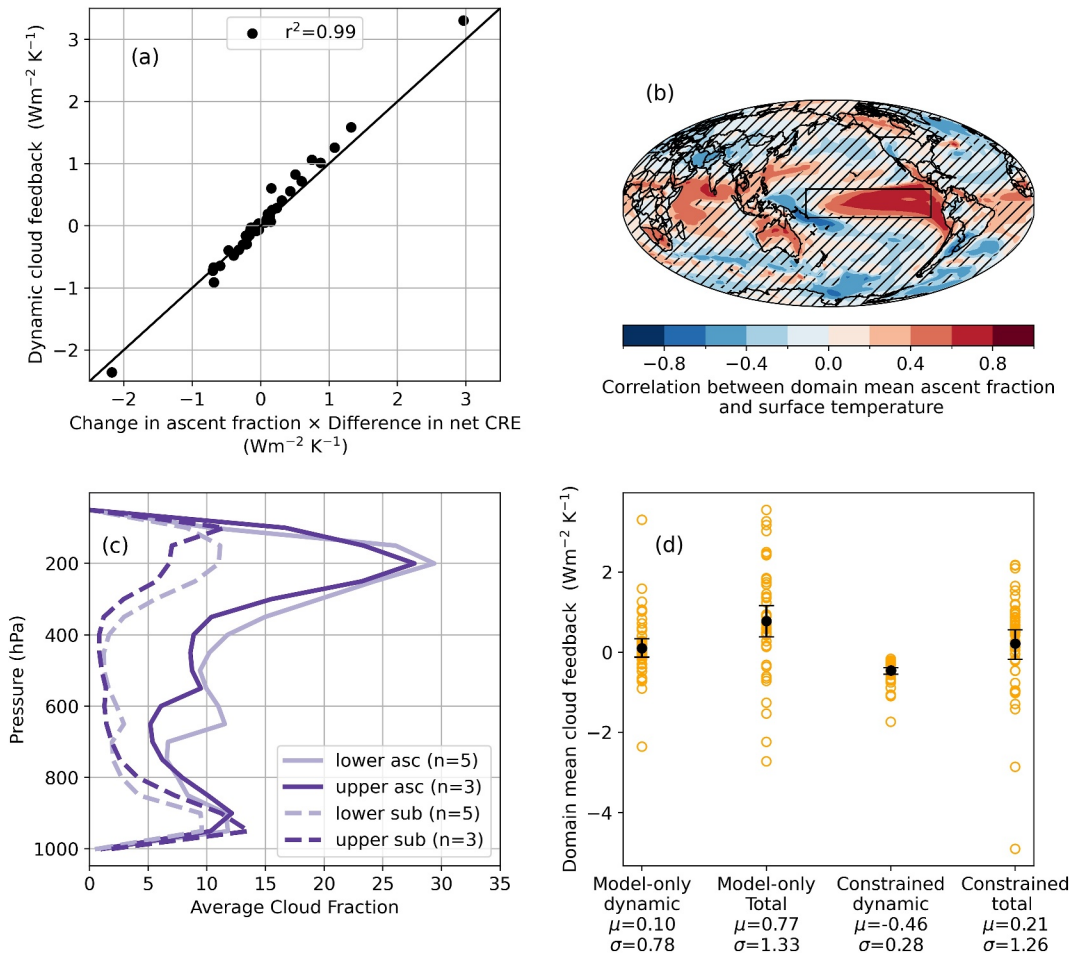

Figure 3. (a) Dynamic cloud feedback as defined by Equation 1 versus the approximate dynamic cloud feedback given by Equation 3 for the equatorial Pacific region for each of the 45 coupled models. (b) Map of gridcell Pearson correlation, across models, of change in domain mean (black box) ascent fraction (K^{-1}) and change in grid-cell surface temperature ($K\ K^{-1}$), where change is relative to global mean surface temperature change. A subset of 26 coupled models are used, denoted by an asterisk in Table S1 in Supporting Information S1. Hatching is where correlations are not significant at the 5% level. (c) Vertical profile of upper and lower tercile average cloud fraction in ascent and subsidence regimes. The number of models (n) in each tercile is listed in the legend. Cloud fraction was interpolated from model level data to a common set of pressure levels. The difference profile between the two circulation regimes is given in Figure S9 in Supporting Information S1. (d) Coupled model dynamic and total regional mean cloud feedbacks when derived directly from the model (first two columns) and when constrained using the observed CRE_{asc}-CRE_{sub} to constrain dynamic cloud feedback component (third and fourth column). Black circle indicates the multi-model mean. Values of the multi-model mean (μ) and inter-model standard deviation (σ) are given below the plot.

$$\underbrace{\int_{-\infty}^{\infty} C(\omega)\delta P(\omega)d\omega}_{\text{dynamic feedback}} \approx \underbrace{\int_{-\infty}^{0} \delta P(\omega)d\omega}_{\textit{ascent frac. change}} \left(\underbrace{\int_{-\infty}^{0} C(\omega)P(\omega)d\omega}_{\textit{ascent CRE}} - \underbrace{\int_{0}^{\infty} C(\omega)P(\omega)d\omega}_{\textit{subsidence CRE}} \right) \quad (3)$$

In fact, there is excellent correlation between dynamic cloud feedback and the terms on the right hand side of this equation (Figure 3a). Models with a positive CRE_{asc}-CRE_{sub} have a positive dynamic feedback and vice versa, and the magnitude of the dynamic cloud feedback increases both with increasing magnitude of CRE_{asc}-CRE_{sub} and with increasing Δ_{asc} (Figure S5 in Supporting Information S1). The reduced spread in the atmosphere-only models is clearly due to the reduced magnitude of changes in ascent fraction for this set of models (Figure S5 in Supporting Information S1). The CRE_{asc}-CRE_{sub} term explains more of the variability than the Δ_{asc} term, but

19448007, 2025, 19, Downloaded from https://agupubs.onlinelibrary.wiley.com/doi/10.1029/2025GL117183 by NICE, National Institute for Health and Care Excellence, Wiley Online Library on [28/10/2025]. See the Terms and Conditions (https://onlinelibrary.wiley.com/terms-and-conditions) on Wiley Online Library for rules of use; OA articles are governed by the applicable Creative Commons License

19448007, 2025, 19, Downloaded from https://agupubs.onlinelibrary.wiley.com/doi/10.1029/2025GL117183 by NICE, National Institute for Health and Care Excellence, Wiley Online Library on [28/10/2025]. See the Terms and Conditions (https://onlinelibrary.wiley.com/terms-and-conditions) on Wiley Online Library for rules of use; OA articles are governed by the applicable Creative Commons License

significantly less than the product of the two (Figure S6 in Supporting Information S1), as models with a large magnitude CRE_{asc}-CRE_{sub} but a weak Δ_{asc} have weaker dynamic cloud feedbacks (Figure S5 in Supporting Information S1). Breaking the CRE_{asc}-CRE_{sub} into its individual SW and LW and ascent and subsidence regime components, correlations with the dynamic cloud feedback are strongest for the SW CRE in ascending regimes, but much weaker than for CRE_{asc}-CRE_{sub} (Figure S7 in Supporting Information S1). This highlights the need for models to accurately capture both SW and LW CREs in both ascent and subsidence regimes, and for improved understanding of the variability in predicted change in ascent fraction.

Figure 3b shows the correlation between Δ_{asc} and surface temperature, clearly highlighting a role of the El Nino-like pattern of warming known to occur in CMIP models (Fox-Kemper et al., 2021). This supports the conclusions of Su et al. (2020) about the importance of SST warming for ascent fraction. Since coupled models are the primary means to assess this SST response to warming, future work will need to increase confidence in the response pattern in order to better constrain this component of cloud feedback.

In order to understand the CRE_{asc}-CRE_{sub} influence on the dynamic feedback we analyze the subset of coupled models that provide a broader set of cloud diagnostics. The equivalent of Figure 2d is reproduced for this subset in Figure S8b in Supporting Information S1. It is clear that this smaller subset still captures the key differences between the tercile groupings in terms of the circulation dependence of net CRE.

For the same subset as Figure S8 in Supporting Information S1, Figure 3c shows average vertical profiles of cloud fraction for the two terciles and for each circulation regime. First, in both ascent and subsidence regimes, high cloud is present, explaining the categorization as a non-low cloud feedback in Figure 1c. In the subsidence regime (dashed lines), the upper tercile models (darker lines) have more low cloud than the lower tercile models (lighter lines), consistent with the more negative SW and net CRE of upper tercile models in this regime (Figure S8 in Supporting Information S1). In the ascent regime (solid lines), low cloud is similar between the tercile sets, but the upper tercile models have less mid-level cloud. A reduction of mid-level cloud is consistent with a less negative SW and net CRE for upper tercile models in the ascent regime. These differences in prevalence of different cloud types amongst models cause differences in net CRE between ascent and subsidence regimes, which causes differences in the dynamic cloud feedbacks.

The model dynamic cloud feedbacks in this region can be constrained by using the observed CRE_{asc}-CRE_{sub} of -7.79 W m^{-2} (Figure 2d) in combination with the approximation given by Equation 2, as shown in Figure 3a. Since the observations show less negative net CRE in subsidence regimes than ascent regimes, the consistent increase in ascent fraction across models leads to a negative dynamic cloud feedback. Removing this component of variability leads to a much smaller inter-model standard deviation of dynamic feedback, reduced to 0.28 W m^{-2} K^{-1} from 0.78 W m^{-2} K^{-1} (though this is in part due to a slight underestimate by the approximation, i.e., the regression line in Figure 3a). This also leads to a more negative multi-model mean value of -0.46 W m^{-2} K^{-1} compared to 0.10 W m^{-2} K^{-1} for the unconstrained calculations. Using the constrained estimate of the dynamic cloud feedback to calculate the total cloud feedback sees a smaller reduction in model-spread (from 1.33 to 1.26 W m^{-2} K^{-1}) due to the co-variation between the dynamic cloud feedback and the non-dynamic cloud feedback. However, the decrease in the mean value remains, with the regional multi-model mean total cloud feedback reduced from 0.77 W m^{-2} K^{-1} to 0.21 W m^{-2} K^{-1}. Accounting for the area of the region, this corresponds to a reduction in the multi-model global mean total cloud feedback of 0.03 W m^{-2} K^{-1}; a small, but not insignificant decrease.

Two models appear as outliers in the constrained total feedback: GISS-E2-2G and CAMS-CSM1-0. It is beyond the scope of this study to assess the robustness of individual models. However, if confidence in these outlier estimates of Pacific cloud feedback was determined to be low, then their removal would result in the constrained total feedback spread (without outliers, $\sigma = 0.89$ W m^{-2} K^{-1}) being a third less than the unconstrained model spread, with the mean estimate then sitting somewhat higher ($\mu = 0.4$ W m^{-2} K^{-1}).

5. Conclusions

In this study, we have presented an investigation of the equatorial Pacific region which shows notably large CMIP6 model spread in cloud feedback. This region is associated with a non-low cloud feedback. Our assessment of cloud profiles highlights that this region has a complex mix of cloud types, with both high and low clouds

19448007, 2025, 19, Downloaded from https://agupubs.onlinelibrary.wiley.com/doi/10.1029/2025GL117183 by NICE, National Institute for Health and Care Excellence, Wiley Online Library on [28/10/2025]. See the Terms and Conditions (https://onlinelibrary.wiley.com/terms-and-conditions) on Wiley Online Library for rules of use; OA articles are governed by the applicable Creative Commons License

present in both ascent and subsidence regimes. The circulation decomposition shows that the difference across models in prevalence of low and mid-level clouds, in this mixed-cloud type region, is fundamental to the estimation of cloud feedback. Although there is a consistent shift across models towards increased occurrence of the ascent regime in response to warming, the sign of the resulting dynamic cloud feedback depends on whether the CRE is more negative in the ascent or the subsidence regime, which models do not agree on.

When we constrain dynamic feedback with the observed dependence of CRE on circulation regime, we find a reduction in the regional total cloud feedback from 0.77 to 0.22 W m^{-2} K^{-1}. Our constraint reduces the model spread in dynamic feedback dramatically, but the reduction of model spread in total feedback is more limited. However, the decomposition method used in this study points to a selection of research pathways for reducing the model spread in total feedback for this notable region:

1. *The current set of AMIP-p4K models are not suitable for understanding cloud feedbacks in this region, so a targeted change in contributing models or an increase in coupled model diagnostics is needed*. Atmosphere-only models, which archive more detailed cloud diagnostics for assessment, significantly underestimate the variability in cloud feedbacks seen in coupled models. Atmosphere-only models underestimate both dynamic and non-dynamic cloud feedback variability. The lack of correlation between atmosphere-only and coupled model cloud feedbacks in this region has already been highlighted by Qin et al. (2022), but in contrast to their hypothesis, we find that, for this region, the correlation between non-dynamic cloud feedbacks is actually smaller than the correlation between dynamic cloud feedbacks. It's possible that a different set of models may better represent the coupled cloud feedback distribution, and would improve on this correlation. But unless a better set can be established in future model intercomparisons, our results highlight the need for more widespread provision of ISCCP simulator output from coupled models in order to facilitate understanding of the non-dynamic, as well as the dynamic, cloud feedback in this region. Whilst our analysis provides an indication of cloud changes involved in the spread, available diagnostics are not sufficient to interpret radiative changes in relation to cloud type changes.
2. *Dynamic cloud feedback depends on the strength of the regional circulation shift towards the ascent regime, with confidence in this requiring a more robust understanding of Pacific cloud-ocean coupling and response*. The shift towards greater ascent in the region with warming is difficult to constrain using observations alone; building confidence in this change requires further analysis of the coupling between the ocean and atmosphere in this region in both coupled models and observations. We show that the shift in ascent regime in models is correlated with the strength of the El Nino-like warming pattern. The results provide additional impetus to improve confidence in this pattern of response simulated by models. The dependence of feedback on the feature highlights the important coupling between clouds and ocean in this region.
3. *Observations should be used to characterize the complex mixing of cloud types in Pacific circulation regimes in order to establish the controls on regime-dependent CRE, which models can then use as a basis for improvement*. Whilst we have used observations to approximately constrain the feedback estimate, this approach cannot correct biases that will occur in the models in response to incorrect radiative effects. Present-day observations are well suited to provide a detailed baseline of cloud types and relationship to CRE and circulation regime, on the monthly and sub-monthly timescales. Model development on the basis of such observational analysis is required in order to improve confidence in the ability of coupled models to simulate cloud feedbacks in the equatorial Pacific.
4. *Targeted assessment of confidence in two outlier estimates would either allow for reduction of the model spread, or elucidate potential extreme cloud feedbacks that researchers should look to understand*. Our constrained total feedback for the Pacific region highlighted two outlier model estimates that are strongly negative. Detailed investigation of these models is warranted to determine confidence in these feedback estimates. If estimates are regarded as unrealistic, the model spread can be further constrained. On the other hand, if these are deemed to be robust estimates, they provide a tool to explore consequences of potentially extreme Pacific cloud feedback.

The above pathways for reducing model spread can improve confidence in our estimates of cloud feedback. However, they have been established through our analysis of spread in model feedbacks and therefore do not represent true uncertainty in the feedback estimate. Aerosol and cloud microphysics are particularly poorly captured physical components in climate models and have been highlighted as knowledge gaps by several recent tropical cloud feedback papers (Gasparini et al., 2023; McKim et al., 2024; Natchiar et al., 2024; Raghuraman

19448007, 2025, 19, Downloaded from https://agupubs.onlinelibrary.wiley.com/doi/10.1029/2025GL117183 by NICE, National Institute for Health and Care Excellence, Wiley Online Library on [28/10/2025]. See the Terms and Conditions (https://onlinelibrary.wiley.com/terms-and-conditions) on Wiley Online Library for rules of use; OA articles are governed by the applicable Creative Commons License

et al., 2024; Sokol et al., 2024). As such, it is also key that future research draws on the cloud measurements by various aircraft and satellite campaigns (e.g., Finney et al., 2024; PERCUSION, 2024; Stevens et al., 2021; Wehr et al., 2023) to understand interaction between aerosol, cloud microphysics, and radiative effect in various circulation regimes.

Conflict of Interest

The authors declare no conflicts of interest relevant to this study.

Data Availability Statement

CMIP6 feedback data is available from Zelinka (2022). Guidance and access for use of other CMIP6 variables is available from PCMDI (2025). ERA5 data are available from the Copernicus Climate Data Store (pressure-level variables: Copernicus Climate Change Service, C. D. S. (2023a) and single-level variables: Copernicus Climate Change Service, C. D. S. (2023b)). MERRA2 data were downloaded from NASA (2025b). JRA55 were downloaded from the NCAR research data archive (Japan Meteorological Agency, 2013). CERES-EBAF data were downloaded from NASA (2025a).

Acknowledgments
PGH and DLF acknowledge funding from the UK Natural Environment Research Council for the CIRCULATES project (Grant NE/T006315/1) and DCMEX project (Grant NE/T006420/1), respectively, and our additional funding under these projects in the form of a CLOUDSENSE synergy grant. The work of MDZ was supported by the U.S. Department of Energy (DOE) Regional and Global Model Analysis program area and was performed under the auspices of the U.S. DOE by Lawrence Livermore National Laboratory under contract DEAC52-07NA27344. We also acknowledge the World Climate Research Programme, which, through its Working Group on Coupled Modelling, coordinated, and promoted CMIP6. We thank the climate modeling groups for producing and making available their model output, the Earth System Grid Federation (ESGF) for archiving the data and providing access, and the multiple funding agencies who support CMIP6 and ESGF. We thank Anna Mackie for her comments on the draft. DLF would like to thank Lawrence Jackson for several useful discussions during the analysis.

References

Alizadeh, O. (2023). A review of ENSO teleconnections at present and under future global warming. *WIREs Climate Change*, *15*(1), e861. https://doi.org/10.1002/wcc.861

Arias, P. A., Bellouin, N., Coppola, E., Jones, R. G., Krinner, G., Marotzke, J., et al. (2021). Technical summary. In *Climate change 2021 – The physical science basis: Working group I contribution to the sixth assesment report of the intergovernmental panel on climate change*. Cambridge University Press. https://doi.org/10.1017/9781009157896.002

Bock, L., & Lauer, A. (2024). Cloud properties and their projected changes in CMIP models with low to high climate sensitivity. *Atmospheric Chemistry and Physics*, *24*(3), 1587–1605. https://doi.org/10.5194/acp-24-1587-2024

Bony, S., Dufresne, J.-L., Le Treut, H., Morcrette, J.-J., & Senior, C. (2004). On dynamic and thermodynamic components of cloud changes. *Climate Dynamics*, *22*(2–3), 71–86. https://doi.org/10.1007/s00382-003-0369-6

Byrne, M. P., & Schneider, T. (2018). Atmospheric dynamics feedback: Concept, simulations, and climate implications. *Journal of Climate*, *31*(8), 3249–3264. https://doi.org/10.1175/jcli-d-17-0470.1

Ceppi, P., Brient, F., Zelinka, M. D., & Hartmann, D. L. (2017). Cloud feedback mechanisms and their representation in global climate models. *WIREs Climate Change*, *8*(4), e465. https://doi.org/10.1002/wcc.465

Copernicus Climate Change Service, C. D. S. (2023a). ERA5 hourly data on pressure levels from 1940 to present. *Copernicus Climate Change Service (C3S) Climate Data Store (CDS)*. https://doi.org/10.24381/cds.bd0915c6

Copernicus Climate Change Service, C. D. S. (2023b). ERA5 hourly data on single levels from 1940 to present. *Copernicus Climate Change Service (C3S) Climate Data Store (CDS)*. https://doi.org/10.24381/cds.adbb2d47

Di Sante, F., Coppola, E., & Giorgi, F. (2021). Projections of river floods in Europe using EURO-CORDEX, CMIP5 and CMIP6 simulations. *International Journal of Climatology*, *41*(5), 3203–3221. https://doi.org/10.1002/joc.7014

Erickson, N. E., & Patricola, C. M. (2023). Future projections of the El Niño—Southern Oscillation and tropical Pacific mean state in CMIP6. *Journal of Geophysical Research: Atmospheres*, *128*(21), e2022JD037563. https://doi.org/10.1029/2022jd037563

Finney, D. L., Blyth, A. M., Gallagher, M., Wu, H., Nott, G. J., Biggerstaff, M. I., et al. (2024). Deep convective microphysics experiment (DCMEX) coordinated aircraft and ground observations: Microphysics, aerosol, and dynamics during cumulonimbus development. *Earth System Science Data*, *16*(5), 2141–2163. https://doi.org/10.5194/essd-16-2141-2024

Forster, P., Storelvmo, T., Armour, K., Collins, W., Dufresne, J.-L., Frame, D., et al. (2021). The Earth's energy budget, climate feedbacks and climate sensitivity. In *Climate change 2021 – The physical science basis: Working group I contribution to the sixth assesment report of the intergovernmental panel on climate change*. Cambridge University Press. https://doi.org/10.1017/9781009157896.009

Fox-Kemper, B., Hewitt, H. T., Xiao, C., Aðalgeirsdóttir, G., Drijfhout, S. S., Edwards, T. L., et al. (2021). Ocean, cryosphere and sea level change. In *Climate change 2021 – The physical science basis: Working group I contribution to the sixth assesment report of the intergovernmental panel on climate change*. Cambridge University Press. https://doi.org/10.1017/9781009157896.011

Gasparini, B., Sullivan, S. C., Sokol, A. B., Kärcher, B., Jensen, E., & Hartmann, D. L. (2023). Opinion: Tropical cirrus – From micro-scale processes to climate-scale impacts. *Atmospheric Chemistry and Physics*, *23*(24), 15413–15444. https://doi.org/10.5194/acp-23-15413-2023

Gelaro, R., McCarty, W., Suárez, M. J., Todling, R., Molod, A., Takacs, L., et al. (2017). The modern-era retrospective analysis for research and applications, version 2 (MERRA-2). *Journal of Climate*, *30*(14), 5419–5454. https://doi.org/10.1175/JCLI-D-16-0758.1

Heede, U. K., & Fedorov, A. V. (2023). Towards understanding the robust strengthening of ENSO and more frequent extreme El Niño events in CMIP6 global warming simulations. *Climate Dynamics*. https://doi.org/10.1007/s00382-023-06856-x

Hersbach, H., Bell, B., Berrisford, P., Hirahara, S., Horányi, A., Muñoz-Sabater, J., et al. (2020). The ERA5 global reanalysis. *Quarterly Journal of the Royal Meteorological Society*, *146*(730), 1999–2049. https://doi.org/10.1002/qj.3803

Hill, P. G., Holloway, C. E., Byrne, M. P., Lambert, F. H., & Webb, M. J. (2023). Climate models underestimate dynamic cloud feedbacks in the tropics. *Geophysical Research Letters*, *50*(15), e2023GL104573. https://doi.org/10.1029/2023gl104573

Japan Meteorological Agency. (2013). *JRA-55: Japanese 55-year reanalysis, daily 3-hourly and 6-hourly data*. Research Data Archive at the National Center for Atmospheric Research. Computational and Information Systems Laboratory. Retrieved from https://climatedataguide.ucar.edu/climate-data/jra-55

Kobayashi, S., Ota, Y., Harada, Y., Ebita, A., Moriya, M., Onoda, H., et al. (2015). The JRA-55 reanalysis: General specifications and basic characteristics. *Journal of the Meteorological Society of Japan. Ser. II*, *93*(1), 5–48. https://doi.org/10.2151/jmsj.2015-001

Loeb, N. G., Doelling, D. R., Wang, H., Su, W., Nguyen, C., Corbett, J. G., et al. (2018). Clouds and the Earth's radiant energy system (CERES) Energy balanced and filled (EBAF) top-of-atmosphere (TOA) Edition-4.0 data product. *Journal of Climate*, *31*(2), 895–918. https://doi.org/10.1175/jcli-d-17-0208.1

Mackie, A., & Byrne, M. P. (2023). Effects of circulation on tropical cloud feedbacks in high-resolution simulations. *Journal of Advances in Modeling Earth Systems*, *15*(5), e2022MS003516. https://doi.org/10.1029/2022ms003516

McKim, B., Bony, S., & Dufresne, J.-L. (2024). Weak anvil cloud area feedback suggested by physical and observational constraints. *Nature Geoscience*, *17*(5), 392–397. https://doi.org/10.1038/s41561-024-01414-4

Meehl, G. A., Senior, C. A., Eyring, V., Flato, G., Lamarque, J.-F., Stouffer, R. J., et al. (2020). Context for interpreting equilibrium climate sensitivity and transient climate response from the CMIP6 Earth system models. *Science Advances*, *6*(26), eaba1981. https://doi.org/10.1126/sciadv.aba1981

Middlemas, E. A., Clement, A. C., Medeiros, B., & Kirtman, B. (2019). Cloud radiative feedbacks and El Niño–Southern Oscillation. *Journal of Climate*, *32*(15), 4661–4680. https://doi.org/10.1175/jcli-d-18-0842.1

NASA. (2025a). *CERES data products: Energy balanced and filled (EBAF)*. Author. Retrieved from https://ceres.larc.nasa.gov/data/

NASA. (2025b). *MERRA2 dataset*. NASA EARTHDATA. Retrieved from https://disc.gsfc.nasa.gov/datasets?project=MERRA-2

Natchiar, S. R. M., Webb, M. J., Lambert, F. H., Vallis, G. K., Morcrette, C. J., Holloway, C. E., et al. (2024). Reduction in the tropical high cloud fraction in response to an indirect weakening of the Hadley Cell. *Journal of Advances in Modeling Earth Systems*, *16*(5), e2023MS003985. https://doi.org/10.1029/2023ms003985

PCMDI. (2025). *CMIP6 guidance for data users*. Lawrence Livermore National Laboratory PCMDI Earth System Model Evaluation Project. Retrieved from https://pcmdi.llnl.gov/CMIP6/Guide/dataUsers.html#3-accessing-model-output

PERCUSION. (2024). ORCESTRA-PERCUSION webpage. Retrieved from https://orcestra-campaign.org/percusion.html

Qin, Y., Zelinka, M. D., & Klein, S. A. (2022). On the correspondence between atmosphere-only and coupled simulations for radiative feedbacks and forcing from CO2. *Journal of Geophysical Research: Atmospheres*, *127*(3), e2021JD035460. https://doi.org/10.1029/2021jd035460

Rädel, G., Mauritsen, T., Stevens, B., Dommenget, D., Matei, D., Bellomo, K., & Clement, A. (2016). Amplification of El Niño by cloud longwave coupling to atmospheric circulation. *Nature Geoscience*, *9*(2), 106–110. https://doi.org/10.1038/ngeo2630

Raghuraman, S. P., Medeiros, B., & Gettelman, A. (2024). Observational quantification of tropical high cloud changes and feedbacks. *Journal of Geophysical Research: Atmospheres*, *129*(7), e2023JD039364. https://doi.org/10.1029/2023jd039364

Sherwood, S. C., Webb, M. J., Annan, J. D., Armour, K. C., Forster, P. M., Hargreaves, J. C., et al. (2020). An assessment of Earth's climate sensitivity using multiple lines of evidence. *Reviews of Geophysics*, *58*(4), e2019RG000678. https://doi.org/10.1029/2019rg000678

Shin, N.-Y., Kug, J.-S., Stuecker, M. F., Jin, F.-F., Timmermann, A., & Kim, G.-I. (2022). More frequent central Pacific El Niño and stronger eastern Pacific El Niño in a warmer climate. *npj Climate and Atmospheric Science*, *5*(1), 101. https://doi.org/10.1038/s41612-022-00324-9

Soden, B. J., & Vecchi, G. A. (2011). The vertical distribution of cloud feedback in coupled ocean-atmosphere models. *Geophysical Research Letters*, *38*(12), L12704. https://doi.org/10.1029/2011gl047632

Sokol, A. B., Wall, C. J., & Hartmann, D. L. (2024). Greater climate sensitivity implied by anvil cloud thinning. *Nature Geoscience*, *17*(5), 398–403. https://doi.org/10.1038/s41561-024-01420-6

Stauffer, C. L., & Wing, A. A. (2022). Properties, changes, and controls of deep-convecting clouds in radiative-convective equilibrium. *Journal of Advances in Modeling Earth Systems*, *14*(6), e2021MS002917. https://doi.org/10.1029/2021ms002917

Stevens, B., Bony, S., Farrell, D., Ament, F., Blyth, A., Fairall, C., et al. (2021). EUREC 4A. *Earth System Science Data*, *13*(8), 4067–4119. https://doi.org/10.5194/essd-13-4067-2021

Su, H., Wu, L., Zhai, C., Jiang, J. H., Neelin, J. D., & Yung, Y. L. (2020). Observed tightening of tropical ascent in recent decades and linkage to regional precipitation changes. *Geophysical Research Letters*, *47*(3), e2019GL085809. https://doi.org/10.1029/2019gl085809

Webb, M. J., Lock, A. P., Bodas-Salcedo, A., Bony, S., Cole, J. N. S., Koshiro, T., et al. (2015). The diurnal cycle of marine cloud feedback in climate models. *Climate Dynamics*, *44*(5–6), 1419–1436. https://doi.org/10.1007/s00382-014-2234-1

Webb, M. J., Senior, C. A., Sexton, D. M. H., Ingram, W. J., Williams, K. D., Ringer, M. A., et al. (2006). On the contribution of local feedback mechanisms to the range of climate sensitivity in two GCM ensembles. *Climate Dynamics*, *27*(1), 17–38. https://doi.org/10.1007/s00382-006-0111-2

Wehr, T., Kubota, T., Tzeremes, G., Wallace, K., Nakatsuka, H., Ohno, Y., et al. (2023). The EarthCARE mission – science and system overview. *Atmospheric Measurement Techniques*, *16*(15), 3581–3608. https://doi.org/10.5194/amt-16-3581-2023

Wing, A. A., Stauffer, C. L., Becker, T., Reed, K. A., Ahn, M., Arnold, N. P., et al. (2020). Clouds and convective self-aggregation in a multimodel ensemble of radiative-convective equilibrium simulations. *Journal of Advances in Modeling Earth Systems*, *12*(9), e2020MS002138. https://doi.org/10.1029/2020ms002138

Wyant, M. C., Bretherton, C. S., Bacmeister, J. T., Kiehl, J. T., Held, I. M., Zhao, M., et al. (2006). A comparison of low-latitude cloud properties and their response to climate change in three AGCMs sorted into regimes using mid-tropospheric vertical velocity. *Climate Dynamics*, *27*(2–3), 261–279. https://doi.org/10.1007/s00382-006-0138-4

Zelinka, M. D. (2022). mzelinka/cmip56_forcing_feedback_ecs: Jun 15, 2022 release. *Zenodo*. https://doi.org/10.5281/zenodo.6647291

Zelinka, M. D. (2024). Cloud feedback maps from CMIP5 and CMIP6 models. *Zenodo*. https://doi.org/10.5281/zenodo.14026963

Zelinka, M. D., & Hartmann, D. L. (2011). The observed sensitivity of high clouds to mean surface temperature anomalies in the tropics. *Journal of Geophysical Research*, *116*(D23), D23103. https://doi.org/10.1029/2011jd016459

Zelinka, M. D., Klein, S. A., & Hartmann, D. L. (2012). Computing and partitioning cloud feedbacks using cloud property histograms. Part I: Cloud radiative kernels. *Journal of Climate*, *25*(11), 3715–3735. https://doi.org/10.1175/jcli-d-11-00248.1

Zelinka, M. D., Klein, S. A., Qin, Y., & Myers, T. A. (2022). Evaluating climate models' cloud feedbacks against expert judgment. *Journal of Geophysical Research: Atmospheres*, *127*(2), e2021JD035198. https://doi.org/10.1029/2021jd035198

Zelinka, M. D., Myers, T. A., McCoy, D. T., Po-Chedley, S., Caldwell, P. M., Ceppi, P., et al. (2020). Causes of higher climate sensitivity in CMIP6 models. *Geophysical Research Letters*, *47*(1), e2019GL085782. https://doi.org/10.1029/2019gl085782

Zelinka, M. D., Zhou, C., & Klein, S. A. (2016). Insights from a refined decomposition of cloud feedbacks. *Geophysical Research Letters*, *43*(17), 9259–9269. https://doi.org/10.1002/2016gl069917

References From the Supporting Information

Klein, S. A., & Jakob, C. (1999). Validation and sensitivities of frontal clouds simulated by the ECMWF model. *Monthly Weather Review*, *127*(10), 2514–2531. https://doi.org/10.1175/1520-0493(1999)127<2514:VASOFC>2.0.CO;2

19448007, 2025, 19, Downloaded from https://agupubs.onlinelibrary.wiley.com/doi/10.1029/2025GL117183 by NICE, National Institute for Health and Care Excellence, Wiley Online Library on [28/10/2025]. See the Terms and Conditions (https://onlinelibrary.wiley.com/terms-and-conditions) on Wiley Online Library for rules of use; OA articles are governed by the applicable Creative Commons License

Shell, K. M., Kiehl, J. T., & Shields, C. A. (2008). Using the radiative kernel technique to calculate climate feedbacks in NCAR's community atmospheric model. *Journal of Climate*, *21*(10), 2269–2282. https://doi.org/10.1175/2007jcli2044.1

Soden, B. J., Held, I. M., Colman, R., Shell, K. M., Kiehl, J. T., & Shields, C. A. (2008). Quantifying climate feedbacks using radiative kernels. *Journal of Climate*, *21*(14), 3504–3520. https://doi.org/10.1175/2007jcli2110.1

Webb, M., Senior, C., Bony, S., & Morcrette, J.-J. (2001). Combining ERBE and ISCCP data to assess clouds in the Hadley Centre, ECMWF and LMD atmospheric climate models. *Climate Dynamics*, *17*(12), 905–922. https://doi.org/10.1007/s003820100157

19448007, 2025, 19, Downloaded from https://agupubs.onlinelibrary.wiley.com/doi/10.1029/2025GL117183 by NICE, National Institute for Health and Care Excellence, Wiley Online Library on [28/10/2025]. See the Terms and Conditions (https://onlinelibrary.wiley.com/terms-and-conditions) on Wiley Online Library for rules of use; OA articles are governed by the applicable Creative Commons License